Effect of Hydrotalcite on the Physical Properties and Drug-Release Behavior of Nanocomposite Hydrogels Based on Poly[acrylic acid-*co*-poly(ethylene glycol) methyl ether acrylate] Gels

Wen-Fu Lee, Yung-Chu Chen

Department of Chemical Engineering, Tatung University, Taipei, Taiwan, Republic of China

Received 3 October 2003; accepted 28 February 2004
DOI 10.1002/app.20936
Published online in Wiley InterScience (www.interscience.wiley.com).

ABSTRACT: A series of nanocomposite hydrogels used for bioadhesive were prepared from acrylic acid, poly(ethylene glycol) methyl ether acrylate, and intercalated hydrotalcite (HT) by photopolymerization. The microstructures of the intercalated HT and sample gels were identified by X-ray diffraction (XRD). The results showed that the swelling ratio for these nanocomposite hydrogels increased with an increase in HT, but the gel strength and adhesive force for these gels decreased with an increase in HT. The XRD results indicated that the exfoliation of intercalated HT was achieved in the xerogels and swollen gels. Finally, the drug-release behaviors for these gels were also examined. © 2004 Wiley Periodicals, Inc. J Appl Polym Sci 94: 692–699, 2004

Key words: hydrogels; nanocomposites; swelling

INTRODUCTION

Bioadhesion is defined as the adhesion of polymers and biological structures and is used for many hard- and soft-tissue applications. The term *bioadhesion* is applied when the substrate is mucus.[1] Some researchers have concluded that polymer characteristics are necessary for bioadhesion: strong hydrogen-bonding groups (—OH and —COOH), strong anionic charge (COO^- and SO^{3-}), high-molecular-weight, sufficient chain flexibility, and surface energy properties favor the spread onto mucus.[2,3] In recent years, drug-delivery systems with bioadhesive drug carriers have become increasingly important because of their ability to adhere to mucosal surfaces of the buccal and skin and thereby increase therapeutic efficiency.[4,5] Typical polymers used as bioadhesive drug carriers include poly(acrylic acid) (PAA), poly(methacrylic acid), carboxymethylcellulose, and hydroxypropyl methylcellulose.[6,7] A wide range of polymers, both natural and synthetic, have been studied for their potential use as bioadhesives.[8–12] Among the investigated polymers, PAA and its lightly crosslinked polymer have been shown to be good bioadhesives because of their hydrophilic nature, negative charge, and high flexibility.[9,13]

Hydrotalcite (HT) is a mineral with positively charged layers and interlayer exchangeable anions.[14,15] Its general composition can be represented as $[M^{II}_{1-X}M^{III}_{X}(OH)_2]^{X+}[A^{q-}_{x/q}nH_2O]$, where M^{II} and M^{III} are divalent and trivalent cations, respectively, and A^{q-} is an exchangeable anion. They are used as inorganic fillers to prepare HT/polymer nanocomposite hydrogels.[16–22]

In the past 10 years, most research on nanocomposites has been focused on the use of silicate clays as nanoparticles.[23,24] These clays have been studied widely because they are naturally occurring minerals that are commercially available and exhibit a platy morphology with a high aspect ratio and considerable cation-exchange capacity. Many reports about the intercalation of organic anions into HT have been published,[25] but relatively few reports have discussed the incorporation of polymers into HT. These studies on HT/polymer nanocomposites have been mainly focused on intercalating, and the performance of these HT nanocomposites has been relatively seldom reported.

Recently, Hsueh and Chen[26] reported HT/polyimide nanocomposites. Their basic idea for producing the HT/polyimide nanocomposites was as follows: at first, the organomodified HT was synthesized by the incorporation of organic anions into HT, followed by polymerization in the interlayer galleries of the HT. After the polymer was generated in the interlayer galleries, the stacking nanolayers of the HT lost their order, and then the nanolayers were exfoliated to disperse in the polymer matrix.

Correspondence to: W.-F. Lee (wflee@ttu.edu.tw).
Contract grant sponsor: Tatung University (Taipei, Taiwan); contract grant number: B90-1413-01.

TABLE I
Feed Compositions, Yield, and *Q* values for Hydrogels

Sample code	AA (mol %)	PEGMEA (mol %)	NMBA (mol %)	IHT (mol %)	DEAP (mol %)	Yield (%)	*Q* (g/g)
P0	90	10	0.1	0	0.1	92	1.28
P1	90	10	0.1	1	0.1	95	1.57
P3	90	10	0.1	3	0.1	93	2.94
P5	90	10	0.1	5	0.1	92	3.92
P7	90	10	0.1	7	0.1	91	5.37
P10	90	10	0.1	10	0.1	94	8.12

IHT - intercalated hydrotalcite.

Nanocomposite hydrogels containing HT were never investigated in the previous reports. In this study, a series of hydrogels used for bioadhesive were prepared from acrylic acid (AA), poly(ethylene glycol) methyl ether acrylate (PEGMEA), and HT by photopolymerization. The effect of the HT content in the nanocomposite hydrogels on the swelling behavior and physical properties in saline solutions was investigated. A further objective was to investigate the effect of HT in these gels on the drug-release behavior for drugs with different charges.

EXPERIMENTAL

Materials

AA and diethoxyacetophenone (DEAP), used as a photoinitiator, were purchased from Fluka Chemical Co. (Buchs, Switzerland). 2-Acryloylamido-2-methyl propane sulfonic acid (AMPS) and *N,N*-dimethylacetamide (DMAc) were purchased from Fluka Chemical. Ultrapure water with a conductivity of 18 S/cm was used in all the experiments. HT was purchased from Aldrich Co. (St. Louis, MO). The anion-exchange capacity of HT was about 350 mequiv/100 g. PEGMEA [number-average molecular weight (M_n) = 454] was purchased from Fluka Chemical. *N,N*-Methylenebisacrylamide (NMBA; M_n = 156), used as a crosslinker, was purchased from Aldrich. Vitamin B2, vitamin B12, crystal violet (CV), and phenol red, used as model drugs, were obtained from Sigma Co. and Fluka, respectively. All the solvents and other chemicals were used as received, except AA, which was purified by vacuum distillation at 29°C and 6 mmHg.

Intercalation of HT

A suspension solution containing 5 g of HT and 3.24 g of AMPS was mixed in 500 mL of DMAc. The suspension solution was stirred at 70°C for 24 h. Then, the intercalated HT was separated by centrifugation and was washed with large volumes of water to remove unintercalated AMPS. The sample was dried in a vacuum oven at 40°C for 3 days.

Preparation of AA/PEGMEA

The monomers (90 mol % AA and 10 mol % of PEGMEA) were weighed and mixed in a 20-mL sample vial. To this solution, 0.1 mol % NMBA, 0.1 mol % DEAP, and intercalated HT in various weight ratios (based on the monomer weight) were then added, and they were mixed thoroughly. The mixture was then injected into the space between two glass plates with a 1-mm silicone rubber as a spacer. Polymerization was carried out through the exposure of the monomer solution to UV irradiation for 10 min. After the gelation was completed, the gel membrane was cut into disks, 10 mm in diameter, immersed in an excess amount of deionized water for 3 days to remove residual components, and dried in a 50°C vacuum oven for 1 day. The feed compositions, yields, and equilibrium swelling ratio (*Q*) of the nanocomposite hydrogels are listed in Table I.

Q measurements

The dried gels were immersed in 10 mL of 0.9 wt % NaCl at 25°C until swelling equilibrium was attained. The weight of the wet sample (W_t) was determined after the removal of surface water via blotting with filter paper. The dry weight (W_d) was determined after the drying of the gel in a vacuum oven for 2 days. The *Q* values of the gels were calculated as follows:

$$Q = (W_t - W_d)/W_d \quad (1)$$

Swelling kinetic measurement

The swelling ratio was obtained via the weighing of the initial and swollen samples at various time intervals. The amount of water absorbed (W_t) was reported as a function of time, and the equilibrium absorption at an infinitely long time was designated W_∞. The following equation was used to calculate the diffusion coefficient (D) for $W_t/W_\infty \leqq 0.8$:[27]

$$W_t/W_\infty = (4/\pi^{0.5})(Dt/L^2)^{0.5} \quad (2)$$

where t is the time and L is the initial thickness of the dried gel. To investigate the diffusion model of the gel, the initial swelling data were fitted to the exponential heuristic equation for $W_t/W_\infty \leqq 0.6$.[28,29]

$$W_t/W_\infty = Kt^n \quad (3)$$

where K is a characteristic constant of the gel and n is a characteristic exponent of the mode transport of the penetrate.

H sensitivity for the nanocomposite hydrogels

A series of pH buffer solutions (citric acid/Na_2HPO_4) were prepared and adjusted to a constant ionic strength of 0.6*M* through the addition of NaCl. The preweighed dried gels were immersed in 10 mL of the buffer solutions to swell. Q of the gels in each pH solution was calculated with eq. (1).

Physical property measurements

The gel strength of these samples was measured by a uniaxial compression experiment with a Lloyd LRX (J. J. Lloyd, Poole, UK) universal tester. Equation (4) was used to calculate the shear modulus (G):

$$\tau = F/A = G(\lambda - \lambda^{-2}) \quad (4)$$

where τ is the compression stress, F is the compression load, A is the cross-sectional area of swollen gels, and λ is the compression strain (L/L_0), where L is the difference of the thickness of deformed gel and initial swollen gel L_0. At low strains, a plot of τ versus $-(\lambda - \lambda^{-2})$ yielded a straight line, the slope of which was G. The effective crosslink density (ρ) was calculated from G and the polymer volume fraction (ν_2) as follows:

$$\rho = G/\nu_2^{1/3}RT \quad (5)$$

where R is the ideal gas constant and T is the absolute temperature.

Assessment of the adhesive force

The force detection system consisted of a precision load cell and a roller with a Lloyd LRX universal tester. The nanocomposite gels were cut (3 cm $\times$ 1 cm $\times$ 1 mm). Then, they were brought into contact with a poly(ethylene terephthalate) (PET) film on the roller. The peel strength was performed at a constant speed of 30 mm/cm, and the force required to fracture the mucoadhesive bond was recorded.

Drug-release experiment

The model solutes used in the drug-release experiments were vitamin B2, vitamin B12, CV, and phenol red. The dry gels were equilibrated in 30 mg of drug/10 mL of deionized water at 25°C for 2 days to load the drugs into the gels. The drug-release experiments were carried out by the transfer of previously incubated drug gels into a 10-mL 0.9 wt % saline solution at 32°C. The gels were repeatedly removed and transferred into a fresh 10-mL saline solution at each fixed time interval. The release drugs were analyzed with a UV spectrophotometer (V530, Jasco, Tokyo, Japan) for vitamin B2 at 445 nm, for vitamin B12 at 360 nm, for CV at 598 nm, and for phenol red at 430 nm.

FTIR analysis

Fourier transform infrared spectra were recorded from pressed KBr pellets containing about 1% HT or intercalated HT with a Horiba FT/IR-720 spectrophotometer (Kyoto, Japan).

X-ray diffraction (XRD) analysis

Powder XRD analyses were performed with a MAC Sienco model M21X X-ray powder diffractometer (Osaka, Japan) with a Cu anode running at 40 kV and 30 mA, scanning from 1 to 13° at 3°/min. The structure of HT was determined at different stages of the nanocomposite synthesis. The HT powders were mounted onto a sample holder with a large cavity, and a smooth surface was obtained by the powders being pressed with a glass plate. Analyses of the HT swollen in the gels were performed by the mixture being spread on a gel membrane disc (50 mm in diameter and 0.5 mm thick) used as a sample holder. It was designed so that a maximum surface could be irradiated at a low angle, giving an optimum intensity to the XRD signal. The nanocomposite plates produced during the molding process had a fairly smooth surface.

RESULTS AND DISCUSSION

Preparation of the nanocomposite hydrogels

The formation of poly[acrylic acid-*co*-poly(ethylene glycol) methyl ether acrylate] [poly(AA-*co*-PEG-MEA)]/HT nanocomposite hydrogels is shown in Scheme 1. HT could not disperse in water. However, intercalated HT through the intercalation of AMPS, which was ionically bonded to the surface of HT by an ion-exchange process, could easily disperse in water. Hence, we successfully prepared a series of nanocomposite hydrogels in aqueous solutions. This scheme implies that the AMPS grafted onto the surface of the HT layer and the intercalated HT was homogeneously

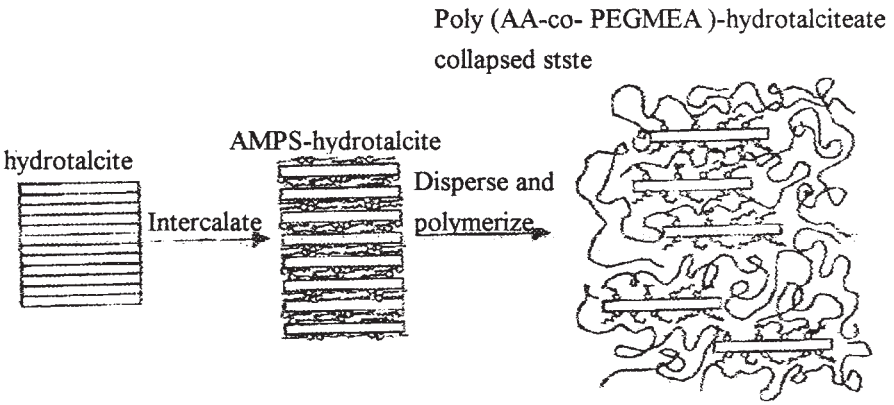

Scheme 1 *In situ* polymerization of poly(AA-*co*-PEGMEA)/HT nanocomposite hydrogels.

dispersed in the poly(AA-*co*-PEGMEA) gel matrix through *in situ* polymerization. Hence, the compatibility between these two phases could be improved (see Scheme 1).

FTIR analysis

The FTIR spectrum of AMPS–HT is shown in Figure 1. Strong absorption peaks of asymmetric and symmetric R—COO^- can be seen at 1610 and 1375 cm^{-1}, respectively. The characteristic absorption peaks of C═O stretching, C═C stretching, N—H bending, asymmetric S═O stretching, and symmetric S═O stretching are at 1658, 1630, 1558, 1205, and 1049 cm^{-1}, respectively. These peaks demonstrate that AMPS was intercalated into HT. A broad absorption peak between 3200 and 3600 cm^{-1} was assigned to O—H stretching of both the hydroxide layers and the interlayer water.

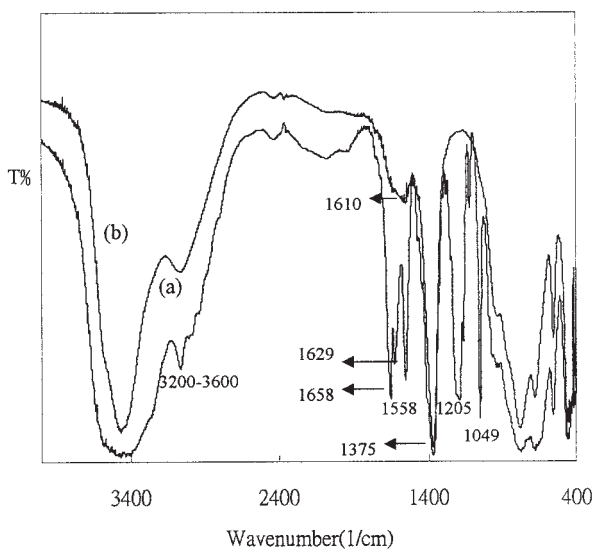

Figure 1 FTIR spectra of (a) intercalated HT and (b) HT.

Identification of the nanocomposite hydrogels

The XRD patterns of various samples are plotted in Figure 2. A typical XRD pattern of HT, with a strong peak corresponding to a basal spacing of 7.49 Å, is shown in Figure 2. After treatment with AMPS, the peak was shifted to a low angle, corresponding to basal spacing of 16.97 Å. This result shows that AMPS was intercalated between the layers during the anion-exchange process, adopting a lateral bilayer structure. For AMPS–HT, two peaks are present at $2\Theta = 5.2°$ and $2\Theta = 11.8°$. This indicates that both AMPS and carbonate groups were present in the interlayer galleries of AMPS–HT. According to Figure 2, the carbonate group content was approximately equal to the AMPS content. The finding perhaps follows from the involvement of fewer CO_2 molecules in the preparation of AMPS–HT. Therefore, AMPS (with one charge) could not exchange a carbonate group (with two charges) completely. After polymerization, both the dried gels and the swollen gels were also analyzed with XRD.

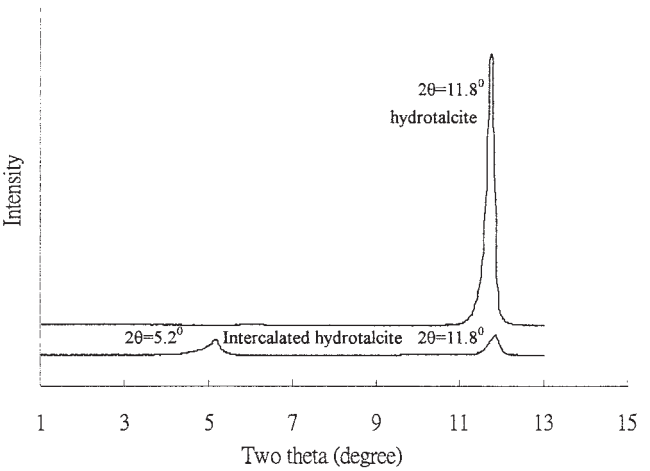

Figure 2 XRD patterns of HT and intercalated HT.

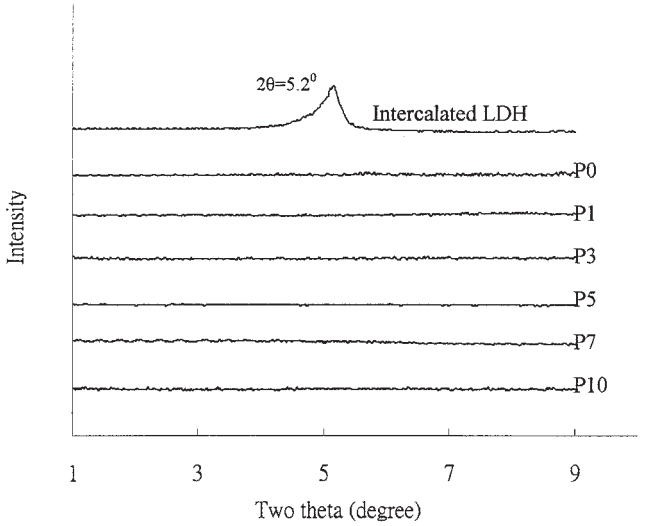

Figure 3 XRD patterns of various dried samples.

The XRD patterns of the various xerogels and swollen gels, shown in Figures 3 and 4, respectively, indicate that the diffraction peak disappeared in all the samples. This result demonstrates that the intercalated HT incorporated into the gels was completely exfoliated.

Effects of intercalated HT on the nanocomposite hydrogel properties

The effects of intercalated HT on some fundamental properties, such as the *Q* value, adhesive force, gel strength, and drug release, for these nanocomposite hydrogels were investigated.

Effect of HT on *Q*

Some characteristics of poly(AA-*co*-PEGMEA)/HT gels with various feed compositions are shown in Table I. The *Q* values for these hydrogels in Table I indicate that the greater the HT content in the gels, the higher the *Q* value of the gels (i.e., P0 < P1 < P3 < P5 < P7 < P10). This is because the original HT, intercalated with hydrophilic AMPS, became a hydrophilic chain; it made the nanocomposite hydrogels more hydrophilic. Hence, the swelling ratio increased with an increase in the content of HT in the gel.

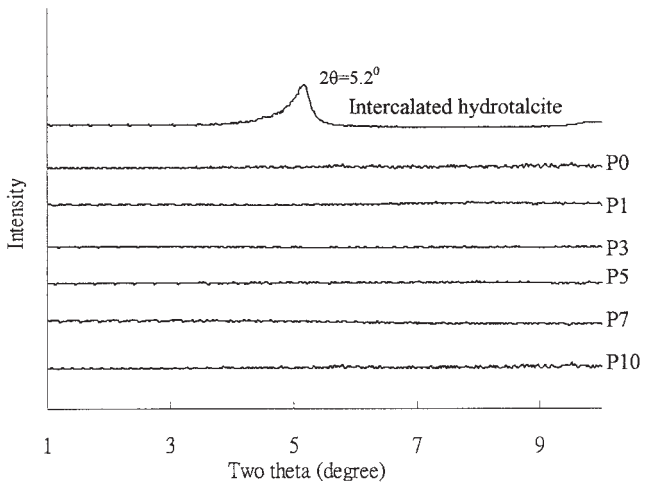

Figure 4 XRD patterns of various swollen samples.

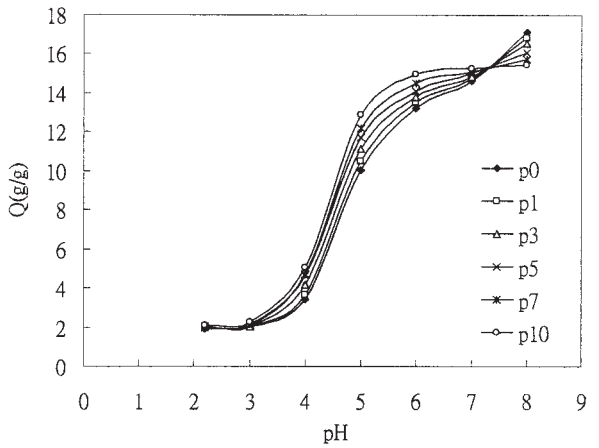

Figure 5 Effect of pH on *Q* for the gels in different pH buffer solutions.

Effect of pH on the swelling ratio

The effect of pH on *Q* for these nanocomposite hydrogels is shown in Figure 5. The swelling ratio increased as the pH increased. However, the gel transition occurring around pH 5 was not obviously affected by the addition of more HT to the gels. Although the gel transition did not change, the gels still possessed an excellent pH response under higher HT loadings. Because AA was the main component in these copolymeric gels, the swelling ratio increased with an in-

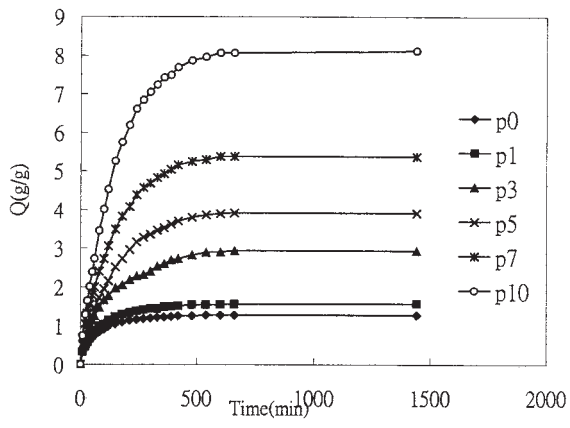

Figure 6 Swelling ratio as a function of time for the hydrogels in a saline solution at 25°C.

TABLE II
Some Fundamental Properties of the Poly(AA-*co*-PEGMEA)/HT Nanocomposite Hydrogels

Sample code	$D \times 10^7$ (cm^2/s)	n	$K \times 10^2$	G (g/cm^2)	$\rho \times 10^{-4}$ (mol/cm^3)	Adhesive force (N/cm^2)
P0	0.26	0.19	7.8	2346 ± 31	1.90 ± 0.27	0.235 ± 0.012
P1	0.33	0.22	6.7	1767 ± 19	1.44 ± 0.24	0.204 ± 0.008
P3	0.44	0.25	5.3	1181 ± 89	1.00 ± 0.22	0.161 ± 0.005
P5	0.51	0.30	4.2	701 ± 41	0.57 ± 0.06	0.136 ± 0.017
P7	0.67	0.34	2.9	630 ± 37	0.52 ± 0.05	0.123 ± 0.012
P10	0.94	0.47	1.1	439 ± 32	0.37 ± 0.04	0.109 ± 0.004

crease in pH. The results shown in this figure indicate that at a lower pH (pH 2), the swelling ratio was the same, but at a higher pH (pH 8), the swelling ratio decreased with an increase in the HT content. Because the carboxylic acid groups were easy to ionize at pH 8, the complexation occurred between anionic AA and cationic HT. Hence, at a higher concentration of HT (P10), the anionic charge density became lower in the gels. At pH 4–6, the swelling ratio increased with an increase in the HT content. This was because the carboxylic acid groups were difficult to ionize at lower pHs.

Effect of HT on the swelling kinetics

The swelling ratios as a function of time for these gels in saline solutions are shown in Figure 6. The n, K, and D values calculated from eqs. (2) and (3) are listed in Table II. The results show that the D values for the gels in saline solutions decreased with increasing HT content in the gel. According to the classification of diffusion mechanisms presented by Alfrey et al.,[30] the results shown in Table II indicate that the transport mechanisms for these nanocomposite hydrogels all belonged to Fickian diffusion ($n < 0.5$).

Effect of HT on the adhesive force

The adhesive forces of the nanocomposite hydrogels are shown in Table II. The adhesive force was determined through the measurement of the force required to break the adhesive surface between the substrate (PET film) and the gels. The results show that the adhesive force for these gels decreased with an increase in the HT content in the gel. This was because the high swelling ratio of the hydrogel diminished the adhesive property of the gel surface. These results explicitly indicate that the higher the HT content in the gel system the greater the hydrophilicity for these gel series.

Effect of HT on the gel strength

The gel strength was assessed from G obtained from eq. (4). The results in Table II indicate that the G and ρ values decreased with an increasing content of HT. These results conform to the results presented by D'Souza et al.,[31] who showed that added hydrophilic montmorillonite in small concentrations led to a decrease in G. They claimed that the result could be attributed to the montmorillonite being well separated and the hydrophilicity. Therefore, we also think that highly hydrophilic AMPS–HT was well dispersed in the gel system. A decrease in G is usually accompanied by a decrease in ρ for hydrogels.

Effect of HT on the fractional drug release of different ionic drugs

Although HT bore positive charges on the surface, a nanocomposite hydrogel still possessed negative

TABLE III
Drug-Loading Amount and Fractional Release of the Nanocomposite Hydrogels

Drug	P0	P1	P3	P5	P7	P10
Vitamin B2						
Loading amount (ppm/g)	814.8	830.6	860.1	884.7	914.2	963.8
Fractional release at 1440 min	69.7%	78.7%	83.6%	86.8%	90.5%	94.7%
CV						
Loading amount (ppm/g)	2448.3	2415.7	2352.6	2296.4	2232.1	2147.5
Fractional release at 1440 min	16.3%	17.1%	19.7%	22.7%	26.8%	34.2%
Pheno red						
Loading amount (ppm/g)	365.5	375.3	392.9	412.9	432.2	464.9
Fractional release at 1440 min	59.1%	56.3%	53.3%	50.2%	48.7%	45.5%
Vitamin B12						
Loading amount (ppm/g)	688.1	657.3	596.9	532.6	477.3	382.3
Fractional release at 1440 min	74.1%	76.1%	78.7%	81.3%	84.2%	88.7%

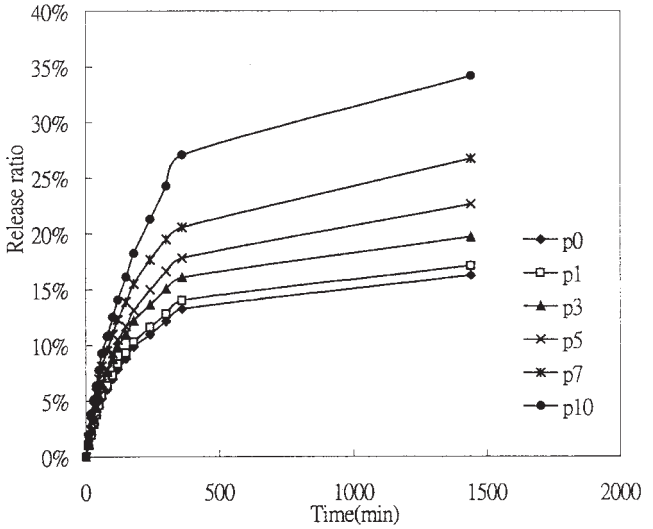

Figure 7 CV release profiles of AA/PEGMEA/HT as a function of time in a saline solution at 32°C.

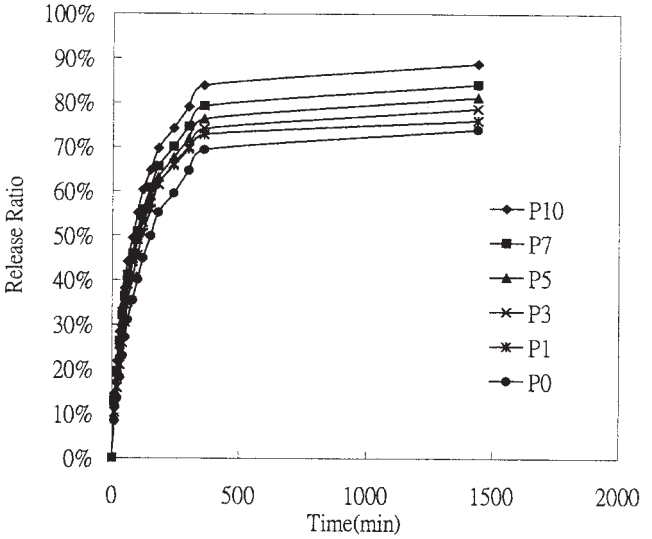

Figure 9 Vitamin B12 release profiles of AA/PEGMEA/HT as a function in a saline solution at 32°C.

charges. This was because a higher concentration of AA made the net charges of the gel remain negative. However, the higher content of HT in the gels decreased the anionic charge density because neutralization occurred between AA and HT. The loading amount and fractional release of the model drugs in these gels are shown in Table III. The drug-release profiles of CV, phenol red, vitamin B12, and vitamin B2 in saline solutions for the nanocomposite hydrogels at 32°C are shown in Figures 7–10, respectively.

The results of cationic CV solutes released from the gels in saline solutions are shown in Figure 7. The higher concentration of HT (P10) lowered the anionic charge density of the gels because of charge neutralization between AA and HT. Hence, the loading amounts of CV in the gels decreased with an increase in HT. On the contrary, the fractional release of CV in the gels increased with an increase in the HT content. This can be observed from the loading amount of CV in the gels (see Table III).

The release profile of anionic phenol red in this nanocomposite hydrogel as a function of time is shown in Figure 8.The charges of the phenol red and this hydrogel were the same, so the loading amounts of phenol red in the gels increased with an increase in HT. On the contrary, the fractional release of phenol red in the gels decreased with an increase in HT. This was because charge repulsion existed between the drug solute and gel; the solute was uneasily loaded into the gel but easily released from gel.

The results of the zwitterionic vitamin B12 solute releasing from the gels in saline solutions are shown in

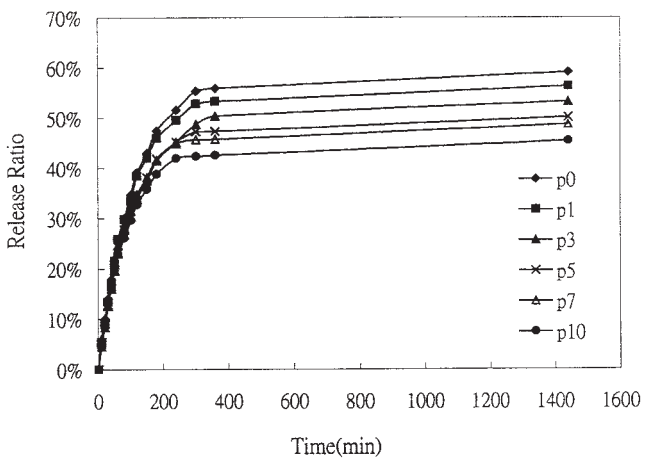

Figure 8 Phenol red release profiles of AA/PEGMEA/HT as a function of time in a saline solution at 32°C.

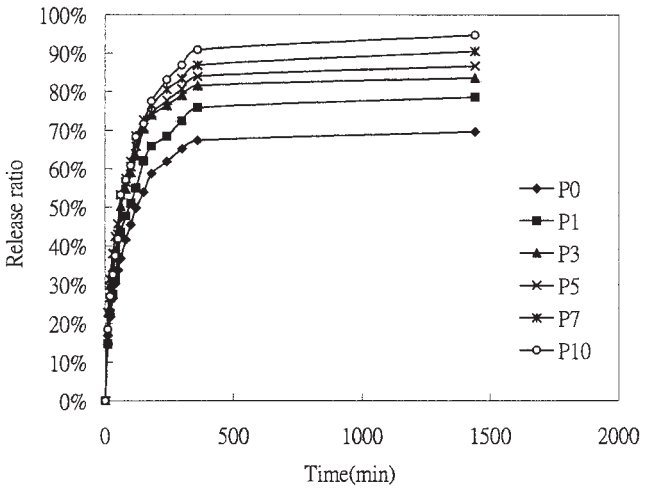

Figure 10 Vitamin B2 release profiles of AA/PEGMEA/HT as a function of time in a saline solution at 32°C.

Figure 9. Vitamin B12 is a zwitterionic drug with an anion (PO_3^-) and a cation (Co^+). For vitamin B12, the negative charge in the gels adsorbed to the positively charged part of the drug molecule. Hence, although the loading amount of vitamin B12 in the gel decreased with an increase in HT, the fractional releases of vitamin B12 in the gels increased with an increase in HT. This was because the nanocomposite hydrogel possessed negative charges, and Co^+ of the vitamin B12 only adsorbed onto the surface of the gels.

The release profile of the uncharged vitamin B2 solute in these gels as a function of time is shown in Figure 10. Vitamin B2 is an uncharged small-molecule drug, so the bonding force between vitamin B2 and the gels was small. Hence, the loading and release of vitamin B2 were mainly affected by the swelling ratio of the hydrogel. The results showed that the loading amount of vitamin B2 in the gels increased with an increase in HT, and the fractional release of vitamin B2 in the gels also increased with an increase in HT.

From these results, we find that the drug-release behavior in poly(AA-*co*-PEGMEA)/HT nanocomposite hydrogels is profoundly affected by the HT content, the charge of the drug solute, and the interaction between the gel and drug solute. These results agree with our previous studies of poly(AA-*co*-PEGMEA)/bentonite hydrogels[32] and charge effects on the drug-release behavior for ionic pH-sensitive hydrogels.[33]

CONCLUSIONS

A poly(AA-*co*-PEGMEA)/HT nanocomposite bioadhesive was successfully synthesized. The following conclusions can be made. The greater the content was of AMPS–HT, the higher the swelling ratio was of the gels. The gel transition at various pH conditions was not affected by the content of AMPS–HT in the gel. The XRD patterns showed that, in the xerogels and the swollen hydrogels, HT was intercalated and exfoliated. Adding AMPS–HT to the gel composition did not enhance the gel strength and crosslinking density of the gels because AMPS–HT was well separated and highly hydrophilic. The adhesive force for these gels decreased with an increase in the HT content in the gel because the high swelling ratio of the hydrogels diminished the adhesive properties of the gel surface. The results for different kinds of drugs showed that the drug-release behaviors were affected by different release factors, including the electrostatic attraction and repulsion between the gels and drugs and the gel networks. If the charges of the drug solute and hydrogel were different, electrostatic attraction existed between them, and the drug was strongly bound in the nanocomposite gels. Therefore, the release ratios were lower. On the contrary, if the charges of the drug solutes and hydrogel were the same, the release ratio of the gel was higher. The swelling ratios of the nanocomposite hydrogels indicated that a gel with a higher swelling ratio could make uncharged drug solutes release through a gel easily.

References

1. Shojaei, A. H.; Li, X. J Controlled Release 1997, 47, 151.
2. Mortazavi, S. A. Int J Pharm 1995, 124, 173.
3. Chickering, D. E.; Mathiowitz, E. J Controlled Release 1995, 34, 251.
4. Florence, A. T.; Jani, P. U. Drug Saf 1994, 10, 233.
5. Hwang, S. J.; Park, H. Crit Rev Ther Drug Carrier Syst 1998, 15, 243.
6. Ahuja, A.; Khar, R. K.; Ali, J. Drug Dev Ind Pharm 1997, 23, 489.
7. Yang, X. J.; Robinson, R. In Biorelated Polymers and Gels: Controlled Release Application in Biomedical Engineering; Okano, T., Ed.; Academic: London, 1998; p 135.
8. Gandhi, R. E.; Robinson, J. R. Ind J Pharm Sci 1988, 50, 145.
9. Ch'ng, H. S.; Park, H.; Kelly, P.; Robinson, J. R. J Pharm Sci 1985, 74, 399.
10. Kriaet, B.; Kissel, T. Int J Pharm 1996, 127, 135.
11. Leung, S. S.; Robinson, J. R. J Controlled Release 1990, 12, 187.
12. Lether, C. M.; Bouwstra, J. A.; Schacht, E. H.; Junginger, H. E. Int J Pharm 1993, 78, 43.
13. Park, H.; Robinson, J. R. Pharm Res 1987, 4, 457.
14. Miyata, S. Clays Clay Miner 1975, 23, 369.
15. Ulibarri, M. A.; Pavlovic, I.; Barriga, C.; Hermosin, M. C.; Cornejo, J. Appl Clay Sci 2001, 18, 17.
16. Sels, B.; Vos, D. D.; Buntinx, M.; Pierard, F.; Mesmaeker, A. K.; Jacobs, P. Nature 1999, 400, 855.
17. Vaccari, A. Catal Today 1998, 41, 53.
18. Yun, S. K.; Pinnavaia, T. J. Chem Mater 1995, 7, 348.
19. Pavan, P. C.; Gomes, G.; Valim, J. B. Microporous Mesoporous Mater 1998, 21, 659.
20. Moreyon, J. E.; De Roy, A.; Forano, C.; Besse, J. P. Appl Clay Sci 1995, 10, 163.
21. Hibino, T.; Tsunashima, A. Chem Mater 1998, 10, 4055.
22. Oriakhi, C. O.; Farr, I. V.; Lerner, M. M. J Mater Chem 1996, 6, 103.
23. Liang, L.; Liu, J.; Gong, X. Langmuir 2000, 16, 9895.
24. Lee, W. F.; Fu, Y. T. J Appl Polym Sci 2003, 89, 3652.
25. Carlino, S. Solid State Ionics 1997, 98, 73.
26. Hsueh, H. B.; Chen, C. Y. Polymer 2003, 44, 1151.
27. Kabra, B. G.; Gehnke, S. W.; Hwang, S. T. J Appl Polym Sci 1991, 42, 2409.
28. Franson, N. M.; Peppas, N. A. J Appl Polym Sci 1983, 28, 1299.
29. Korsmeyer, R. W.; Merrwall, E. W.; Peppas, N. A. J Polym Sci Part B: Polym Phys 1986, 24, 109.
30. Alfery, T.; Gurnee, F.; Lloyd, W. G. J Polym Sci Part C: Polym Symp 1966, 12, 249.
31. Xia, X.; Yih, J.; D'Souza, N. A.; Hu, Z. Polymer 2003, 44, 3389.
32. Lee, W. F.; Chen, Y. C. J Appl Polym Sci 2004, 91, 2934.
33. Lee, W. F.; Chiu, R. J. Mater Sci Eng C 2002, 20, 161.